

# Application of evolved gas analysis to cold-cap reactions of melter feeds for nuclear waste vitrification

Carmen P. Rodriguez<sup>a</sup>, Jaehun Chun<sup>a,\*</sup>, Michael J. Schweiger<sup>a</sup>, Albert A. Kruger<sup>b</sup>, and Pavel R. Hrna<sup>a,c</sup>

<sup>a</sup>*Pacific Northwest National Laboratory, Richland, WA 99352, USA*

<sup>b</sup>*U.S. Department of Energy Office of River Protection, Richland, WA 99352, USA*

<sup>c</sup>*Division of Advanced Nuclear Engineering, Pohang University of Science and Technology, Pohang, Republic of Korea*

## ABSTRACT

In the vitrification of nuclear wastes, the melter feed (a mixture of nuclear waste and glass-forming and modifying additives) experiences multiple gas-evolving reactions in an electrical glass-melting furnace. We employed the thermogravimetry-gas chromatography-mass spectrometry (TGA-GC-MS) combination to perform evolved gas analysis (EGA). Apart from identifying the gases evolved, we performed quantitative analysis relating the weighed sum of intensities of individual gases linearly proportional with the differential thermogravimetry. The proportionality coefficients were obtained by three methods based on the stoichiometry, least squares, and calibration. The linearity was shown to be a good first-order approximation, in spite of the complicated overlapping reactions.

**Keywords:** Cold-cap reactions, Evolved gas analysis, Nuclear waste vitrification, Kinetic models

---

\* Corresponding author. Tel.: +1 509 372 6257; fax: +1 509 372 5997.  
E-mail address: jaehun.chun@pnnl.gov (J. Chun).

## 1. Introduction

The cold-cap is a floating layer of melter feed, or glass batch, on a pool of molten glass in a continuous electrical glass-melting furnace, a melter. For vitrifying nuclear waste glass [1–3], the feed, a mixture of waste with glass-forming and -modifying additives, is charged onto the cold-cap that covers 90–100% of the melt surface. As the feed progresses through the cold-cap, it undergoes chemical reactions and phase transitions through which it is converted to molten glass that moves from the cold cap into the melt pool.

The nuclear waste (i.e., mixed hazardous waste) contains 40 to 60 elements forming water-soluble salts, amorphous gels, and crystalline minerals. The conversion to glass proceeds over a wide range of temperatures (~100–1100°C) spanning the formation of molten salts that react with feed solids, turning them into intermediate products and ultimately the glass-forming melt. Various cold-cap reactions evolve gases that escape from the cold cap through open pores. A small fraction of residual gases can be trapped in the glass-forming melt and cause foaming. Foam reduces the heat transfer from molten glass into the cold cap, decreasing the rate of melting. Understanding the cold-cap reactions over the temperature range of the conversion process helps formulate melter feeds for higher production rates, and hence an enhanced efficiency of the vitrification facility, by minimizing the overlap between the gas-evolving reactions and the formation of a continuous glass-forming melt.

Gas-evolving cold-cap reactions release chemically bonded water and produce  $\text{NO}_x$ ,  $\text{O}_2$ , and  $\text{CO}_x$  from reactions of nitrates with organics and reactions of nitrates, nitrites and carbonates with solids [4–16]. Pokorný et al. [3] modeled the kinetics of the gas-evolving cold-cap reactions using data from non-isothermal thermogravimetric analysis (TGA). Their model described the overall reaction rate as a sum of mutually independent  $n$ th-order reaction kinetics with the Arrhenius rate coefficients. For simplification, they neglected interactions between consecutive reactions and the complex responses of multicomponent molten salts and other reactants. Chun et al. [17] used a similar approach to develop a kinetic model for heat-consuming cold-cap reactions from simultaneous differential scanning calorimetry (DSC)-TGA data. It should be noted that reaction peaks

identified in both approaches could result from the combination of sub-reactions at a very similar temperature range unless the mixtures are treated at a wide range of heating rates.

The TGA- and DSC-based kinetic models provide phenomenological descriptions of the cold-cap reactions. Given the complexity of nuclear waste feeds and glass batches in general, these methods do not identify chemical species involved. Neither does the evolved gas analysis (EGA), but it, at least, allows the gases evolved to be recognized. Previous informative, yet semi-quantitative, EGA studies [18,19] analyzed off-gases from a laboratory-scale furnace without attempting to determine contributions of each gas to the mass losses. In this study, we correlated the mass loss rate from TGA with the well-resolved fluxes of gases as detected by gas chromatography-mass spectrometry (GC-MS) to obtain a quantitative EGA. The resulting model provides contributions of individual gases to mass losses associated with the feed-to-glass conversion.

The following section defines the basic concepts and relationships needed for the modeling. Sections 3 and 4 describe the experiments and the results. Section 5 discusses the performance and applicability of the model and the identification of chemical characteristics (i.e., evolved gas species and possible reactants) for the ‘apparent’ reactions in the previous kinetic studies.

## 2. Background for modeling

Assuming that the mass loss of the batch is only associated with gas evolution reactions [3], the mass of the feed at time  $t$  is

$$m(t) = m_I - m_{\text{loss}}(t) = m_I - \sum_{j=1}^{N_g} m_j(t) \quad (1)$$

where  $m_I$  is the initial mass,  $m_{\text{loss}}$  is the mass loss,  $m_j$  is the mass loss associated with the  $j$ th off-gas,  $N_g$  is the number of gas species, and  $t$  is the time. This assumption is reasonable for alkali-borosilicate batches for temperatures  $< \sim 800^\circ\text{C}$ ; above this temperature, volatilization losses become appreciable.

Differentiating Eq. (1) with respect to time yields

$$-\frac{dm(t)}{dt} = \sum_{j=1}^{N_g} \frac{dm_j(t)}{dt} \quad (2)$$

For analysis with GC-MS, the flux of  $j$ th gas species, represented via intensity,  $I_j$ , is proportional to the number of molecular ions (or instrumentally induced charges or produced current). For quantitative analysis, we postulated, as an approximation, that the mass change rate of the  $j$ th off-gas is linearly proportional to the  $j$ th off-gas intensity.

Thus,

$$\frac{dm_j(t)}{dt} = F_j I_j(t + \Delta t) \quad (3)$$

where  $F_j$  is the  $j$ th off-gas proportionality coefficient and  $\Delta t$  is the time lag, assumed to be invariant, between the TGA signal and the MS detector reading due to the off-gas transfer to the MS detector. The dimension of  $F_j$  is such that the  $F_j I_j$  product has an appropriate [mass/time] unit.

Generally, various factors need to be considered for a correlation between TGA and MS signals such as flow patterns in the TGA chamber and carrier gas flow rates [20,21]. Eq. (3) would not be applicable in the presence of interfering experimental artifacts and a strong coupling of the reaction evolving the  $j$ th off-gas with other reactions, e.g., the gas consumed by other reactions. However, the implementation of GC column (i.e., the affinity of gas species to a stationary phase inside the GC column) and small volume of the GC injector, as well as an equipped mass flow controller, may sufficiently reduce the broadening of the MS peaks to allow Eq. (3) to be a reasonable approximation (see Sections 3.2 and Fig. 2).

Combining Eqs. (2) and (3), one obtains

$$-\frac{dm(t)}{dt} = \sum_{j=1}^{N_g} F_j I_j(t + \Delta t) \quad (4)$$

This equation correlates the mass loss rate from TGA with the weighted sum of intensities from MS via  $N_g$  coefficients. Eq. (4) can be integrated obtaining

$$\Delta m = \sum_{j=1}^{N_g} F_j \int_0^{t_f} I_j(t + \Delta t) dt \quad (5)$$

where  $\Delta m = m_I - m_{\text{loss}}$  (see Eq. (1)) is the total mass of gases evolved (equal to the mass loss of the feed) and  $t_f$  is the time at which the evolution of batch gases was complete.

Obviously,  $\Delta m$  is the sum of masses of individual batch gases, thus

$$\Delta m = \sum_{j=1}^{N_g} \Delta m_j \quad (6)$$

where  $\Delta m_j$  is the sample mass change caused by  $j$ th gas evolution. By Eq. (5),

$$\Delta m_j = F_j \int_0^{t_f} I_j(t + \Delta t) dt \quad (7)$$

Similar to calibrations performed for quantitative and semi-quantitative MS analyses [22], the integrated intensity can be compared with the mass change of a solid sample that releases the  $j$ th gas in a single reaction, obtaining

$$\Delta m_j = C_j \int I_j(t) dt \quad (8)$$

where  $C_j$  is the  $j$ th gas calibration coefficient; the range of integration is determined by the start and end of the gas-evolving reaction. Three different subsamples are typically analyzed to minimize experimental errors. Unless there is a strong kinetic coupling between gas-evolving reactions of the feed,  $F_j = C_j$  from Eqs. (7) and (8).

### 3. Experimental

#### 3.1. Feed materials

Table 1 shows the melter feed composition used in this study. As described earlier [3,17,23], this feed, denoted as A0, was formulated to vitrify a high-alumina high-level waste to produce glass of the following composition (with mass fractions in parentheses): SiO<sub>2</sub> (0.305), Al<sub>2</sub>O<sub>3</sub> (0.240), B<sub>2</sub>O<sub>3</sub> (0.152), Na<sub>2</sub>O (0.096), CaO (0.061), Fe<sub>2</sub>O<sub>3</sub> (0.059), Li<sub>2</sub>O (0.036), Bi<sub>2</sub>O<sub>3</sub> (0.011), P<sub>2</sub>O<sub>5</sub> (0.011), F (0.007), Cr<sub>2</sub>O<sub>3</sub> (0.005), PbO (0.004), NiO (0.004), ZrO<sub>2</sub> (0.004), SO<sub>3</sub> (0.002), K<sub>2</sub>O (0.001), MgO (0.001), and ZnO (0.001). This glass was designed for the Hanford Tank Waste Treatment and Immobilization Plant, currently under construction at the Hanford Site in Washington State, USA [24]. As described by Schweiger et al. [23], the simulated melter feed was prepared in the form of slurry that was dried, crushed into powder, and placed in an oven at ~ 105°C overnight.

### 3.2. TGA-GC-MS system

In the study, we used a simultaneous TGA-GC-MS couple system NETZSCH STA 449 F1 Jupiter® - Simultaneous TGA-DSC instrument simultaneously coupled to the Agilent 7890A gas chromatograph equipped with an Agilent 5975C single quadrupole mass spectrometer. Evolved gases move directly from the TGA chamber (under atmospheric pressure) to the GC-MS via heated transfer tubing (keeping at 200°C). Evolved gases were filled into the GC sampling loop, injected into the GC column every minute, eluted with Helium gas, and reached to the MS detector. Unlike a conventional capillary coupling, the stationary phase in the GC, along with a small injection volume, provides different interactions with each gas in the mixture, allowing a better resolution. Equipped with a mass flow controller, no significant broadening of the peaks in the MS is, therefore, expected in the TGA-GC-MS coupling.

The TGA microbalance was calibrated with weight standards, following the manufacturer guidelines. To minimize leaks, impurities, and residues from TGA/GC and peripheral setups (e.g., pumps and valves), multiple runs were performed with the heating rate of 10 K min<sup>-1</sup> from 50°C to 1200°C.

The EGA was performed by placing 61.7 mg of A0 feed into a platinum crucible. After loading the crucible into the TGA furnace, the instrument was stabilized, following manufacturer guidelines, by flowing helium through the system a couple of times. Next, to reduce background noises, the GC-MS instrument was stabilized by flowing helium through the system for 2–3 hours and then run for about 10 minutes. The open crucible with the sample was heated at 10 K min<sup>-1</sup> from 50°C up to 1200°C. Helium was used as both a purge gas, (at a constant flow rate of 20 ml min<sup>-1</sup>) and protective gas (at a constant flow rate of 40 ml min<sup>-1</sup>). The GC injector was set to splitless mode. The GS-CarbonPLOT capillary column, specially designed for low molecular weight gas molecules, such as N<sub>2</sub>, CH<sub>4</sub>, CO<sub>2</sub>, N<sub>2</sub>O, and H<sub>2</sub>O, was 30 m long and 320 μm in inner diameter and possessed a 3-μm film thickness. The GC-MS instrument ran under a helium atmosphere with a constant column flow rate of 1.5 ml min<sup>-1</sup>. The valve box, containing a 250 μl sampling loop inside, was kept at 200°C. To avoid possible condensation, the GC column and the connecting valve was kept at 200°C and held at this temperature for ~ 70 minutes (corresponding to ~ 750°C) to ensure the completion of

possible reactions. The reproducibility was checked at the optimized setting conditions (i.e., temperature, size of crucible, and flow rates specified) over multiple times.

The National Institute of Standards and Technology (NIST) mass spectral database, containing a collection of electron ionization mass spectra for various molecular species, was employed to identify evolved gases. For the MS, ionization energy was set to 20 eV, the scan range  $m/z$  (mass-to-charge ratio) was 10–100, and the the GC-MS interface was set to 280°C.

## 4. Results

### 4.1. Evolution of gases

Fig. 1 shows the normalized mass loss (TG), its time derivative (DTG), and intensity from GC-MS. The four gases, CO<sub>2</sub>, H<sub>2</sub>O, NO, and O<sub>2</sub>, were identified by matching observed  $m/z$  patterns in MS with the NIST spectroscopy library database.

As shown in Fig. 1(b), the major gases are CO<sub>2</sub> and H<sub>2</sub>O with significant overlapping. The minor NO peak and the tiny O<sub>2</sub> peak coincide with the major peak of CO<sub>2</sub> while H<sub>2</sub>O continues to evolve. The first DTG peak at ~10 minutes (~ 150°C), which did not occur in our previous study [3], is caused by the evolution of excess water accumulated by absorption of moisture.

To match the DTG and GC-MS temperature scales, data were smoothed with spline interpolation and a 1.5-min time lag was applied. The time lag of the off-gas transfer from TGA to MS detector corresponds to the 1.5-ml min<sup>-1</sup> flow rate through the 30-m column of 320- $\mu$ m inner diameter.

### 4.2. Proportionality coefficients

In principle, proportionality coefficients ( $F_j$ 's) can be determined using three methods: (A) the usage of Eq. (7) with  $\Delta m_j$  values determined by stoichiometry of the batch chemicals, (B) fitting of Eq. (4) to DTG and EGA data using the least squares regression, and (C) the usage of Eq. (8) and replacement of  $F_j$ 's by the  $C_j$  coefficients determined from EGA of a simple solid involving a single gas-evolving reaction.

Each of these methods has a drawback. The first method ('stoichiometry' method) can be applied only if no gases are evolved from, or absorbed by, the sample before the EGA analysis was performed. This is a condition likely met by the reactions evolving NO and O<sub>2</sub>, because these gases originated from nitrates and nitrites that are sufficiently stable, but not by reactions evolving H<sub>2</sub>O and CO<sub>2</sub> as discussed in section 4.2.1.

The second method ('least squares' method) is limited to gas evolving reactions that are independent and their peaks do not coincide. As Fig. 1(b) indicates, this is not the case for the NO and O<sub>2</sub> peaks, which are eclipsed by the CO<sub>2</sub> peak.

The third method ('calibration' method) should work for all gases but needs to be checked with the other two methods.

The common source of uncertainty for all three methods is that the small size of the sample containing a large number of components can cause composition deviations. The following subsections describe the application of the three methods to experimental data.

#### 4.2.1. Stoichiometry method

The amounts of gases that evolve from the batch chemicals listed in Table 1 during the vitrification process can be obtained based on the stoichiometry. The *j*th gas-to-glass mass fraction can then be expressed as,  $\Gamma_{B,j} = \Delta m_{B,j} / (m_B - \Delta m_B)$ , where  $m_B$  is the mass of chemicals batched to make glass,  $\Delta m_{B,j}$  is the total mass of *j*th gas evolved from chemicals batched, and  $\Delta m_B$  is the total mass of all gases evolved. Thus,  $\Gamma_{B,CO_2} = 0.0558$ ,  $\Gamma_{B,NO} = 0.0041$ ,  $\Gamma_{B,O_2} = 0.0023$ , and  $\Gamma_{B,H_2O} = 0.2871$ , which sums to the total mass loss from batched chemical per glass  $\Gamma_B = 0.3493$ .

By the TGA, the actual mass loss from dry feed per unit mass of glass,  $\Gamma_F$  was by 21% lower than that from the precursors. This value,  $\Gamma_F = 0.2751$ , is based on the sample mass difference between the room temperature and ~730°C, the temperature at which the liberation of the batch gases was no longer detected by the TGA. As temperature increased above 800°C, the mass loss resumed because of melt volatilization and oxygen released from redox reactions of Fe<sub>2</sub>O<sub>3</sub> and CrO<sub>4</sub><sup>2-</sup>.

The total gas-to-dry feed mass fraction is thus  $\psi = \Gamma_F / (1 + \Gamma_F) = 0.2158$ . The average value of  $\psi$  from a previous study [3] was 0.2023±0.0029. The experimental value of the

loss-on-ignition obtained from an independently prepared feed was 0.1917. These values are close considering uncertainties associated with feed preparation, aging, and the small sample size used for thermal analysis.

Generally,  $\Gamma_{B,j}$  consists of three contributions, the fraction released or absorbed during sample preparation ( $\Gamma_{j,p}$ ), the fraction released or absorbed during sample storage ( $\Gamma_{j,s}$ ), and the fraction released during conversion reactions ( $\Gamma_{j,h}$ ); thus,

$$\Gamma_{B,j} = \Gamma_{j,p} + \Gamma_{j,s} + \Gamma_{j,h}.$$

As stated above,  $F_j$ s for NO and O<sub>2</sub> can be safely estimated based on the stoichiometry of the batch chemicals, i.e.,  $\Gamma_{j,p} = \Gamma_{j,s} = 0$  ( $j = \text{NO}$  and O<sub>2</sub>) and  $\Gamma_{B,j} = \Gamma_{j,h}$  ( $j = \text{NO}$  and O<sub>2</sub>). However, not all bonded water from the batched chemicals is retained in the dry feed. Some originally bonded water was liberated during feed preparation, especially drying, due to water-releasing chemical reactions. Also some water was re-absorbed from the atmosphere during dry feed storage or slowly lost by continuing reactions. Hence,  $\Gamma_{\text{H}_2\text{O},p}$  and  $\Gamma_{\text{H}_2\text{O},s}$  can be substantial. The absorption of CO<sub>2</sub> from the atmosphere promoted by the high alkali nature of the feed is highly probable. Therefore, the  $\Gamma_{\text{CO}_2,s}$  is likely to be positive.

We start with an assumption that the only sources of CO<sub>2</sub> in the sample are the oxalate and carbonates from the batch and the difference between  $\Gamma_B$  and  $\Gamma_F$  is solely attributed to H<sub>2</sub>O. Then the  $j$ th gas-to-dry feed mass fraction for gases other than H<sub>2</sub>O is  $\psi_j = \Gamma_{B,j} / (1 + \Gamma_F)$ ; thus,  $\psi_{\text{CO}_2} = 0.0437$ ,  $\psi_{\text{NO}} = 0.0032$ , and  $\psi_{\text{O}_2} = 0.0018$ . Since the fraction of H<sub>2</sub>O makes the difference between the sum of these three values and the total ( $\psi$ ), we obtain  $\psi_{\text{H}_2\text{O}} = 0.1670$ .

Because, by definition,  $\psi_j = \Delta m_j / m$ , Eq. (7) yields

$$F_j = \frac{\psi_j m_{TGA}}{\int_0^{t_f} I_j dt} \quad (9)$$

where  $m_{TGA}$  is the sample mass used in TGA. With the stoichiometric  $\psi_j$  values for CO<sub>2</sub>, NO, and O<sub>2</sub> and the TGA-based value for H<sub>2</sub>O, Eq. (9) yields the stoichiometry-based  $F_j$  values shown in Table 2 ('stoichiometry'). Fig. 2(a) displays the evolution rates of

individual gases as well as the sum of all gases, which is compared with mass loss rate by the TGA. While the EGA and TGA curves nearly coincide at  $t < \sim 30$  min, indicating that the  $F_{\text{H}_2\text{O}}$  coefficient has an acceptable value, a predominant lack of fit for the  $\text{CO}_2$  peak indicates that the  $\text{CO}_2$  fraction in the sample was probably higher than that which came from the batch chemicals, and thus the  $F_{\text{CO}_2}$  coefficient is underestimated.

#### 4.2.2. Least squares method

The underestimated  $F_{\text{CO}_2}$  coefficient imposes a question on the assumption that batch chemicals were the only sources of  $\text{CO}_2$  in the sample. But, without this assumption, it is impossible to obtain  $F_j$ s for  $\text{H}_2\text{O}$  and  $\text{CO}_2$  independently based on stoichiometry.

Alternatively,  $F_{\text{H}_2\text{O}}$  and  $F_{\text{CO}_2}$  coefficients can be obtained by using the least squares analysis while leaving  $F_{\text{NO}}$  ( $= 2.97 \times 10^{-7}$ ) and  $F_{\text{O}_2}$  ( $= 6.93 \times 10^{-8}$ ) from the stoichiometry method unchanged. The analysis minimizes the value of the expression:

$$\sum_{i=1}^n \left[ \frac{dm(t)}{dt} + \sum_{j=1}^{N_g} F_j I_j(t + \Delta t) \right]^2 \quad (10)$$

where  $n$  is the number of GC-MS data measured (typically less than that from TGA). The optimized values of the  $F_{\text{H}_2\text{O}}$  and  $F_{\text{CO}_2}$  coefficients are listed in Table 2, showing that the fitted  $F_{\text{CO}_2}$  value is higher than that obtained based on the feed stoichiometry. As Fig. 2(b) demonstrates, the EGA and TGA curves based on the coefficients by the least squares method nearly coincide.

#### 4.2.3. Calibration method

Additionally, the calibration based on simple solids producing  $\text{H}_2\text{O}$  and  $\text{CO}_2$  (i.e.,  $C_{\text{H}_2\text{O}}$  and  $C_{\text{CO}_2}$ ) can approximate  $F_{\text{H}_2\text{O}}$  and  $F_{\text{CO}_2}$  coefficients. Fig. 3 displays the TGA-GC-MS analysis for a  $\text{CaCO}_3$  sample (evolving  $\text{CO}_2$  by the reaction  $\text{CaCO}_3 \rightarrow \text{CaO} + \text{CO}_2$ ) heated at  $10 \text{ K min}^{-1}$ . The value  $C_{\text{CO}_2} = 1.51 \times 10^{-7}$  was obtained from averaged for 3.3-, 5.2-, and 5.7-mg samples. Similarly, with calcium oxalate monohydrate ( $\text{CaC}_2\text{O}_4 \cdot \text{H}_2\text{O} \rightarrow \text{CaC}_2\text{O}_4 + \text{H}_2\text{O}$ ) for 3.0-, 4.8-, and 9.3-mg samples,  $C_{\text{H}_2\text{O}} = 1.14 \times 10^{-6}$

was obtained. These coefficients are compared in Table 2 with the coefficients based on stoichiometry (assuming zero external source of CO<sub>2</sub>, NO, and O<sub>2</sub>) and the least squares analysis (assuming zero external sources or sinks of NO and O<sub>2</sub>).

Fig. 2(c) shows the comparison between DTG and EGA curves using the calibration method. Similar to the least squares method, the discrepancy between the EGA and TGA is minimal even at the major overlapping range (i.e., 30-50 minutes). Also, in spite of the differences of the CO<sub>2</sub> mass evolved relative to the batch stoichiometry ( $\Delta_{\text{CO}_2}$ ), the differences of the total mass evolved relative to the TGA ( $\Delta_{\text{total}}$ ) was insignificant.

Fig. 4 provides an additional evaluation of the proportionality assumption in terms of the instantaneous mass change rate by DTG versus the gas evolution rate by EGA showing that these rates nearly coincide except for values around sharp major peaks where EGA data were not detected.

## 5. Discussion

### 5.1. Coefficient invariance

The results summarized in Table 2 imply that the following assumptions are likely to be valid:

- a)  $F_j$  coefficients are virtually independent of temperature
- b)  $F_j$  coefficients are independent of the gas source
- c) The time lag,  $\Delta t$ , implemented in Eq. (3), is virtually constant over the gas-evolution temperature interval.

The near-match of DTG and EGA peak shapes and positions and the lack of peak broadening are consequences of these propositions, in addition to the minimization of experimental artifacts, such as the condensation of evolved gases and impurities from TGA/GC and peripheral setups. Thus, Eq. (4) is suitable as a first order approximation. The proportionality assumptions stated are based on limited amount of data but may be sufficient for comparing the cold-cap reactions that occur during the vitrification of melter feeds formulated for nuclear wastes.

### 5.2. Identification of batch reactions

The previously reported TGA analysis [3] was solely focused on reaction kinetics. Identifying the gases by EGA provides a step toward the identification of the gas-evolving reactions for individual TGA peaks with the ultimate goal of understanding the reaction mechanisms. As Fig. 1 shows, the TGA peaks for individual gases overlap. By EGA results, the TGA peaks below 400°C mainly correspond to H<sub>2</sub>O evolution and the TGA peaks above 400°C correspond to CO<sub>2</sub> evolution while H<sub>2</sub>O is still evolving.

The missing information is the identification of the reactants and the products. While the EGA can add the chemical characteristics to the peaks identified in the TGA, it cannot differentiate between individual reactions that produce the same gas. An exact number of H<sub>2</sub>O evolving reactions would be more than the number of peaks in Fig. 1. Based on feed composition in Table 1, H<sub>2</sub>O is released from hydroxides, acids, and hydrates, such as NaOH, H<sub>3</sub>BO<sub>3</sub>, Al(OH)<sub>3</sub>, Fe(OH)<sub>3</sub>, Zn(NO<sub>3</sub>)<sub>2</sub>·4H<sub>2</sub>O, Zr(OH)<sub>4</sub>·0.654H<sub>2</sub>O, Na<sub>2</sub>C<sub>2</sub>O<sub>4</sub>·3H<sub>2</sub>O, and Bi(OH)<sub>3</sub>. NaOH is likely to react with more acidic feed chemicals, such as H<sub>3</sub>BO<sub>3</sub> and Al(OH)<sub>3</sub> to form, on the slurry (pH ~ 11-12) preparation. Similarly, the TGA peaks above 400°C are associated with reactions of carbonates, such as Li<sub>2</sub>CO<sub>3</sub>, NiCO<sub>3</sub>, and Na<sub>2</sub>C<sub>2</sub>O<sub>4</sub> that may partly turn to Na<sub>2</sub>CO<sub>3</sub> on heating.

The identification of individual reactions requires additional information, preferably by performing TGA and EGA for combinations of selected feed components, as Wilburn and Thomasson [4–7] have done for commercial glass batches. Additionally, x-ray diffraction provides a limited source of data by providing information about crystalline solids. However, most of the feed solids are amorphous gels.

## 6. Conclusions

An understanding of the cold-cap reactions, although still incomplete, has been enhanced by the quantitative EGA via TGA-GC-MS combination, thus adding the identification of evolving gases to the phenomenological kinetic model based on change of sample mass or heat. Three different methods based on stoichiometry, least squares, and calibration give rise to the linear relationship that correlates the overall mass loss rate from TGA to the production rate for individual gases from EGA, which puts the gas

generation on a quantitative basis. Future work could include identifying cold-cap reactions, including the reactants and the products.

### **Acknowledgements**

This work was supported by the Department of Energy's Waste Treatment & Immobilization Plant Federal Project Office. Pavel Hрма was also partially supported by the World Class University program through the National Research Foundation of Korea funded by the Ministry of Education, Science and Technology (R31 - 30005). The authors are grateful to Drs. Dong-Sang Kim and Ekkehard Post for insightful discussions and instructions on the TGA-GC-MS setup and tests, respectively. Pacific Northwest National Laboratory is operated by Battelle Memorial Institute for the U.S. Department of Energy under contract DE-AC05-76RL01830.

### **References**

- [1] R. Pokorný, P. Hрма, Mathematical modeling of cold cap, *J. Nucl. Mater.* 429 (2012) 245–256.
- [2] P. Hрма, A.A. Kruger, R. Pokorný, Nuclear waste vitrification efficiency: cold cap reactions, *J. Non-Cryst. Solids* 358 (2012) 3559–3562.
- [3] R. Pokorný, D.A. Pierce, P. Hрма, Melting of glass batch: Model for multiple overlapping gas-evolving reactions, *Thermochim. Acta* 541 (2012) 8–14.
- [4] F.W. Wilburn, C.V. Thomasson, The application of differential thermal analysis and thermogravimetric analysis to the study of reactions between glass-making materials. Part 1. The sodium carbonate–silica system, *J. Soc. Glass Technol.* 42 (1958) 158T–175T.
- [5] C.V. Thomasson, F.W. Wilburn, The application of differential thermal analysis and thermogravimetric analysis to the study of reactions between glass-making materials. Part 2. The calcium carbonate–silica system with minor batch additions, *Phys. Chem. Glasses* 1 (1960) 52–69.

- [6] F.W. Wilburn, C.V. Thomason, The application of differential thermal analysis and thermogravimetric analysis to the study of reactions between glass-making materials. Part 3. The sodium carbonate–silica system, *Phys. Chem. Glasses* 2 (1961) 126–131.
- [7] F.W. Wilburn, C.V. Thomason, The application of differential thermal analysis and differential thermogravimetric analysis to the study of reactions between glass-making materials. Part 4. The sodium carbonate–silica–alumina system, *Phys. Chem. Glasses* 4 (1963) 91–98.
- [8] F.W. Wilburn, S.A. Metcalf, R.S. Warburton, Differential thermal analysis, differential thermogravimetric analysis, and high temperature microscopy of reactions between major components of sheet glass batch, *Glass Technol.* 6 (1965) 107–114.
- [9] E. Bader, Thermoanalytical investigation of melting and fining of Thüringen laboratory glassware, *Silikattechnik* 29 (1978) 84–87.
- [10] J. Mukerji, A.K. Nandi, K.D. Sharma, Reaction in container glass batch, *Ceram. Bull.* 22 (1979) 790–793.
- [11] O. Abe, T. Utsunomiya, Y. Hoshino, The reaction of sodium nitrate with silica, *Bull. Chem. Soc. Jpn.* 56 (1983) 428–433.
- [12] T.D. Taylor, K.C. Rowan, Melting reactions of soda-lime-silicate glasses containing sodium sulfate, *J. Am. Ceram. Soc.* 66 (1983) C227–228.
- [13] M. Lindig, E. Gehrman, G.H. Frischat, Melting behavior in the system  $\text{SiO}_2\text{-K}_2\text{CO}_3\text{-CaMg}(\text{CO}_3)_2$  and  $\text{SiO}_2\text{-K}_2\text{CO}_3\text{-PbO}$ , *Glastech. Ber.* 58 (1985) 27–32.
- [14] C.A. Sheckler, D.R. Dinger, Effect of particle size distribution on the melting of soda-lime-silica glass, *J. Am. Ceram. Soc.* 73 (1990) 24–30.
- [15] K.S. Hong, R.E. Speyer, Thermal analysis of reactions in soda-lime-silicate glass batches containing melting accelerants: I. One- and two-component systems, *J. Am. Ceram. Soc.* 76 (1993) 598–604.
- [16] K.S. Hong, S.W. Lee, R.E. Speyer, Thermal analysis of reactions in soda-lime-silicate glass batches containing melting accelerants: II. Multicomponent systems, *J. Am. Ceram. Soc.* 76 (1993) 605–608.

- [17] J. Chun, D.A. Pierce, R. Pokorný, P. Hrna, Cold-cap reactions in vitrification of nuclear waste glass: experiments and modeling. *Thermochim. Acta* 559 (2013) 32–39.
- [18] P.A. Smith, J.D. Vienna, P. Hrna, The effects of melting reactions on laboratory-scale waste vitrification. *J. Mater. Res.* 10 (1995) 2137–2149.
- [19] J. Matyáš, P. Hrna, D.-S. Kim, Melt Rate Improvement for High-Level Waste Glass, PNNL-14003, Pacific Northwest National Laboratory, Richland, Washington, 2002.
- [20] B. Roduit, J. Baldyga, M. Maciejewski, A. Baiker, Influence of mass transfer on interaction between thermoanalytical and mass spectrometric measured in combined thermoanalyzer-mass spectrometer systems, *Thermochim. Acta* 295 (1997) 59–71.
- [21] M. Maciejewski, A. Baiker, Quantitative calibration of mass spectrometric signals measured in coupled TA-MS system, *Thermochim. Acta* 295 (1997) 95–105.
- [22] C.-A. Craig, K.E. Jarvis, L.J. Clarke, An assessment of calibration strategies for the quantitative and semi-quantitative analysis of calcium carbonate matrices by laser ablation-inductively coupled plasma-mass spectroscopy (LA-ICP-MS). *J. Anal. At. Spectrom.* 15 (2000) 1001–1008.
- [23] M.J. Schweiger, P. Hrna, C.J. Humrickhouse, J. Marcial, B.J. Riley, N.E. TeGrotenhuis, Cluster formation of silica particles in glass batches during melting, *J. Non-Cryst. Solids* 356 (2010) 1359–1367.
- [24] P.R. Hrna, M.J. Schweiger, B.M. Arrigoni, C.J. Humrickhouse, J. Marcial, A. Moody, C. Rodriguez, R.M. Tate, B. Tincher, Effect of Melter-Feed-Makeup on Vitrification Process, PNNL-18374, Pacific Northwest National Laboratory, Richland, Washington, 2009.

## Tables

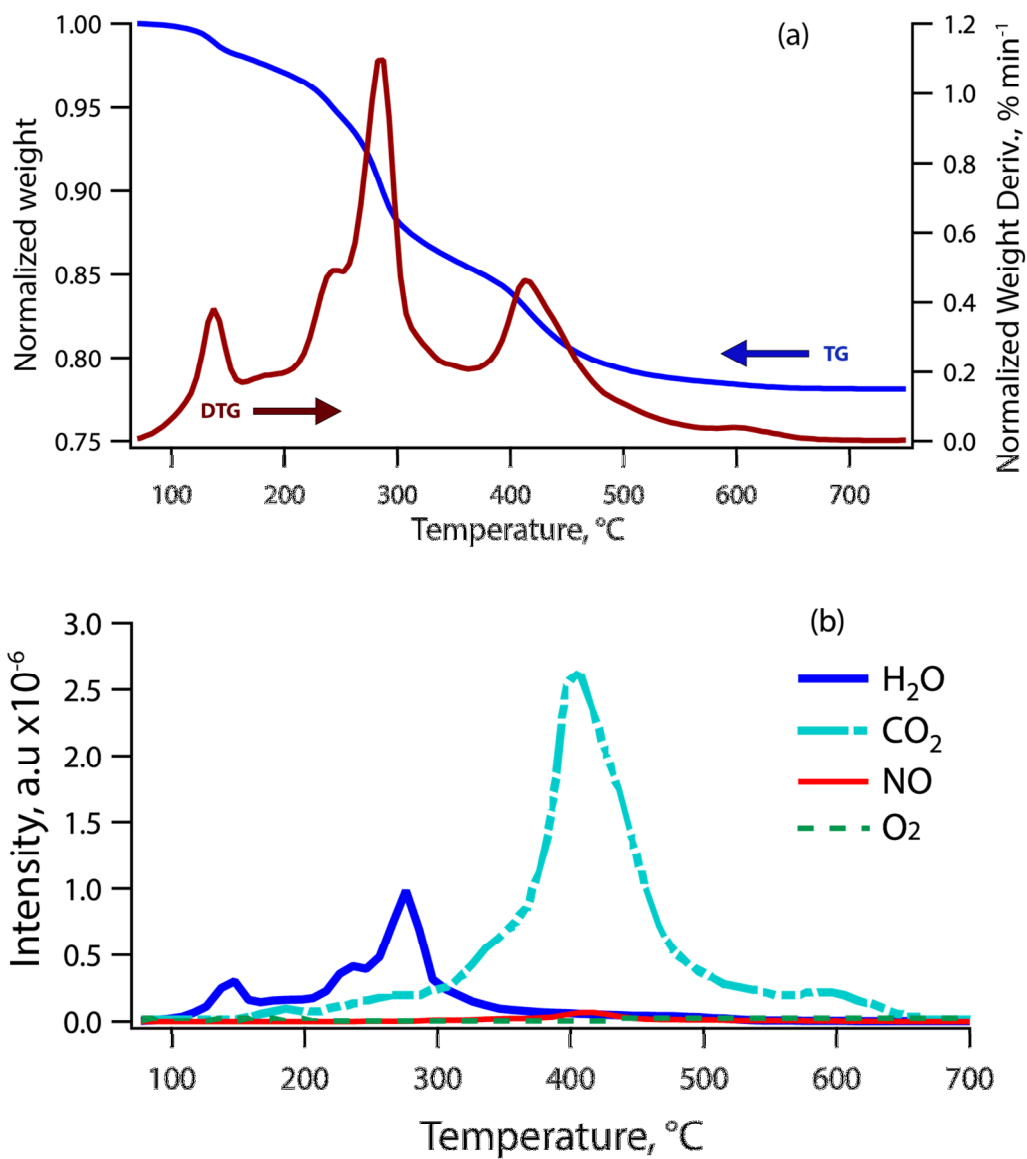
Table 1. Melter feed composition for high-alumina high-level waste in g kg<sup>-1</sup> glass.

Chemicals	Mass (g)
Al(OH) <sub>3</sub>	367.50
H <sub>3</sub> BO <sub>3</sub>	269.83
CaO	60.80
Fe(OH) <sub>3</sub>	73.83
Li <sub>2</sub> CO <sub>3</sub>	88.30
Mg(OH) <sub>2</sub>	1.70
NaOH	99.53
SiO <sub>2</sub>	305.03
Zn(NO <sub>3</sub> ) <sub>2</sub> ·4H <sub>2</sub> O	2.67
Zr(OH) <sub>4</sub> ·0.654H <sub>2</sub> O	5.50
Na <sub>2</sub> SO <sub>4</sub>	3.57
Bi(OH) <sub>3</sub>	12.80
Na <sub>2</sub> CrO <sub>4</sub>	11.13
KNO <sub>3</sub>	3.03
NiCO <sub>3</sub>	6.33
Pb(NO <sub>3</sub> ) <sub>2</sub>	6.17
Fe(H <sub>2</sub> PO <sub>2</sub> ) <sub>3</sub>	12.43
NaF	14.73
NaNO <sub>2</sub>	3.40
Na <sub>2</sub> C <sub>2</sub> O <sub>4</sub> ·3H <sub>2</sub> O	1.30
Total	1349.6

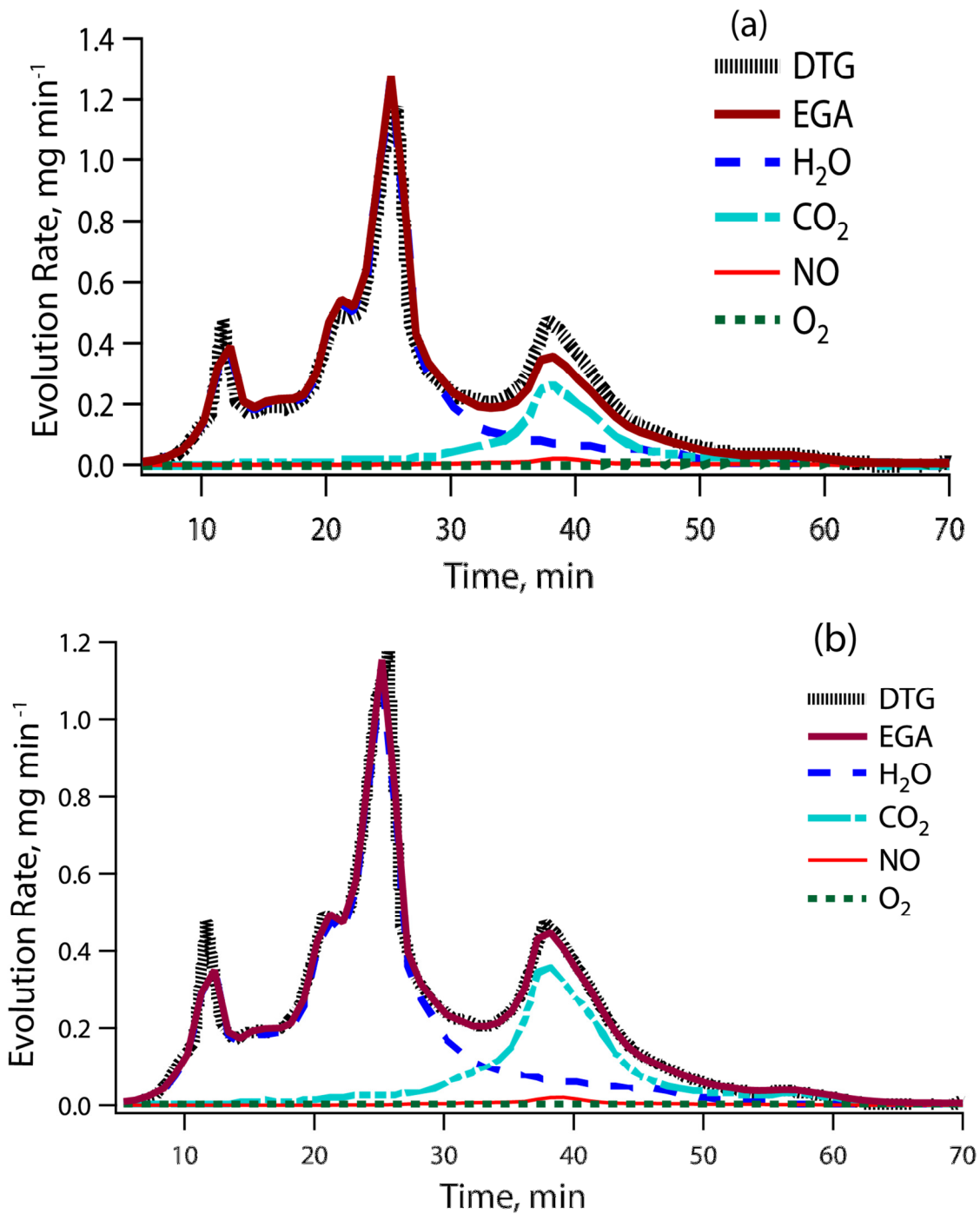
Table 2. Proportionality coefficients of H<sub>2</sub>O and CO<sub>2</sub> and comparison based on three methods;  $\Delta_{\text{CO}_2}$  and  $\Delta_{\text{total}}$  denote the percentage of differences for CO<sub>2</sub> mass evolved (relative to the batch stoichiometry) and for the total mass evolved (relative to the TGA), respectively.

Method	$F_{\text{H}_2\text{O}}$	$F_{\text{CO}_2}$	$\Gamma_{\text{CO}_2}$	$\Delta_{\text{CO}_2}$	$\Delta_{\text{total}}$
Stoichiometry	$1.28 \times 10^{-6}$	$9.85 \times 10^{-8}$	0.0437	0 %	0 %
Least squares	$1.15 \times 10^{-6}$	$1.36 \times 10^{-7}$	0.0603	38.4 %	-0.14 %
Calibration	$1.14 \times 10^{-6}$	$1.51 \times 10^{-7}$	0.0652	49.6 %	0.22 %

**Fig. 1.** (a) Dry feed TGA performed at  $10\text{ K min}^{-1}$ : TG is the normalized weight loss and DTG is the normalized weight derivative (b) As-recorded intensity from GC-MS.



**Fig. 2.** Gas evolution rates for gaseous species by TGA and GC-MS with the proportionality coefficients from three different methods: (a) stoichiometry method, (b) least squares method, and (c) calibration method.



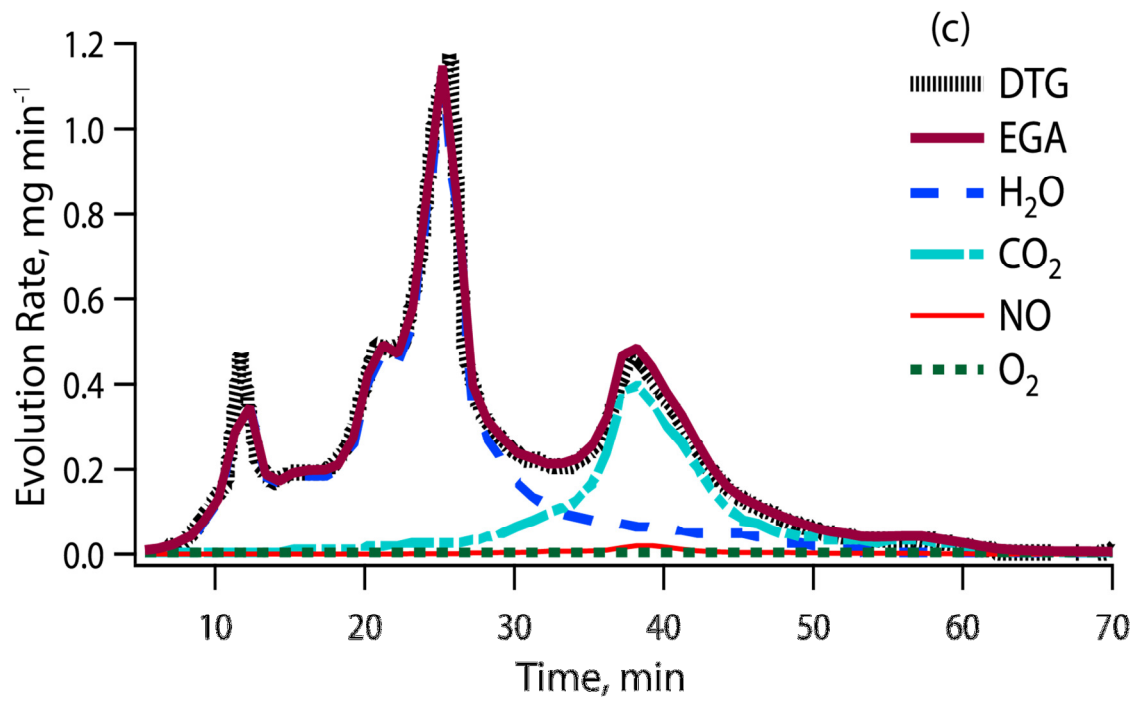


**Fig. 3.** Thermal decomposition of  $\text{CaCO}_3$  heated at  $10 \text{ K min}^{-1}$ : (a) mass loss % and (b) normalized weight derivative (from TGA) with the intensity (from MS) as a function of temperature.

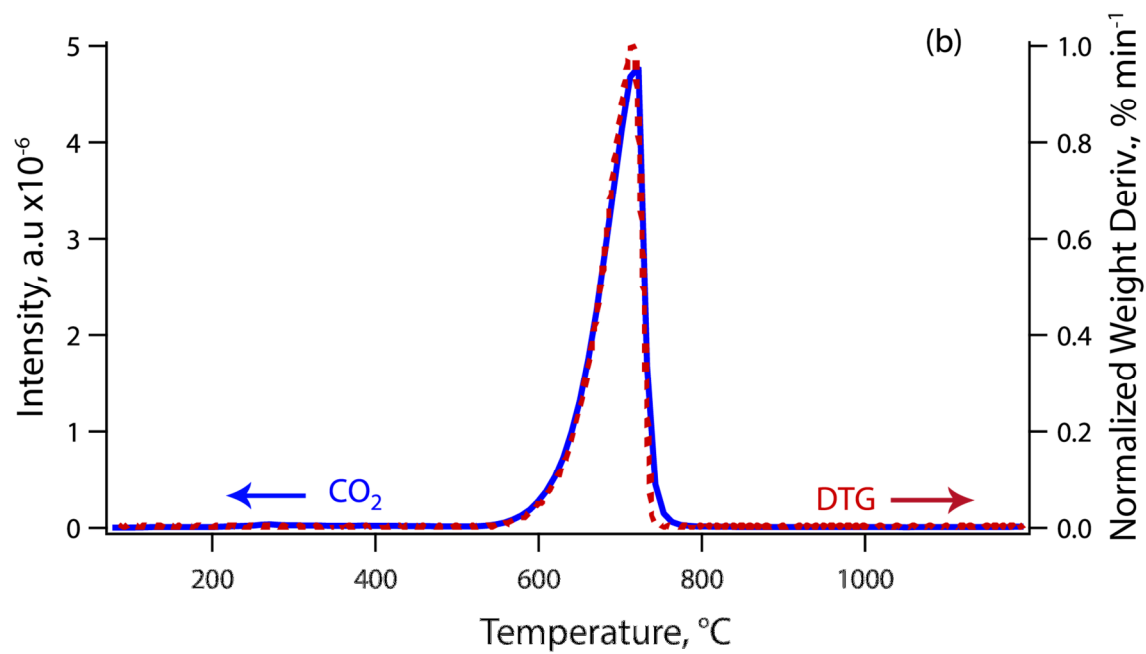
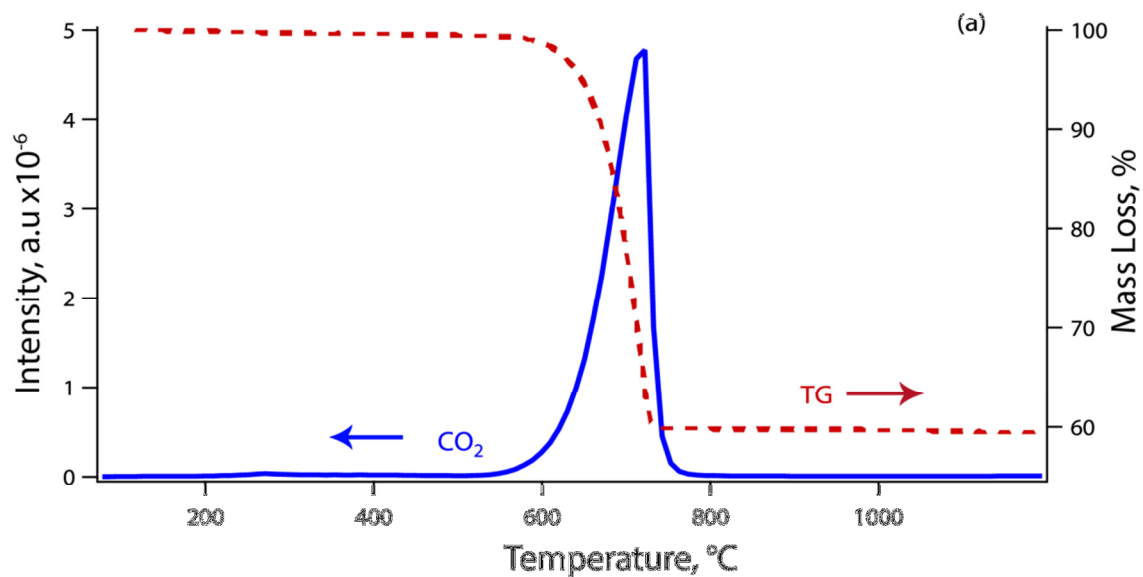


**Fig. 4.** Instantaneous mass loss rate versus gas evolution rate estimated by stoichiometry, least square, and calibration methods; the line represents identity.

